

MODELING THE COMBINED EFFECTS OF DETERMINISTIC AND STATISTICAL STRUCTURE FOR OPTIMIZATION OF REGIONAL MONITORING Annual Report

Vernon F. Cormier, et al.

**Physics Department
University of Connecticut
2152 Hillside Road, U-3046
Storrs, CT 06269-3046**

30 June 2014

Technical Report

APPROVED FOR PUBLIC RELEASE; DISTRIBUTION IS UNLIMITED.



**AIR FORCE RESEARCH LABORATORY
Space Vehicles Directorate
3550 Aberdeen Ave SE
AIR FORCE MATERIEL COMMAND
KIRTLAND AIR FORCE BASE, NM 87117-5776**

DTIC COPY

NOTICE AND SIGNATURE PAGE

Using Government drawings, specifications, or other data included in this document for any purpose other than Government procurement does not in any way obligate the U.S. Government. The fact that the Government formulated or supplied the drawings, specifications, or other data does not license the holder or any other person or corporation; or convey any rights or permission to manufacture, use, or sell any patented invention that may relate to them.

This report was cleared for public release by the 377 ABW Public Affairs Office and is available to the general public, including foreign nationals. Copies may be obtained from the Defense Technical Information Center (DTIC) (<http://www.dtic.mil>).

AFRL-RV-PS-TR-2014-0163 HAS BEEN REVIEWED AND IS APPROVED FOR PUBLICATION IN ACCORDANCE WITH ASSIGNED DISTRIBUTION STATEMENT.

//SIGNED//

Dr. Robert Raistrick
Project Manager, AFRL/RVBYE

//SIGNED//

Glenn M. Vaughan, Colonel, USAF
Chief, Battlespace Environment Division

This report is published in the interest of scientific and technical information exchange, and its publication does not constitute the Government's approval or disapproval of its ideas or findings.

REPORT DOCUMENTATION PAGE				Form Approved OMB No. 0704-0188	
Public reporting burden for this collection of information is estimated to average 1 hour per response, including the time for reviewing instructions, searching existing data sources, gathering and maintaining the data needed, and completing and reviewing this collection of information. Send comments regarding this burden estimate or any other aspect of this collection of information, including suggestions for reducing this burden to Department of Defense, Washington Headquarters Services, Directorate for Information Operations and Reports (0704-0188), 1215 Jefferson Davis Highway, Suite 1204, Arlington, VA 22202-4302. Respondents should be aware that notwithstanding any other provision of law, no person shall be subject to any penalty for failing to comply with a collection of information if it does not display a currently valid OMB control number. PLEASE DO NOT RETURN YOUR FORM TO THE ABOVE ADDRESS.					
1. REPORT DATE (DD-MM-YYYY) 30-06-2014		2. REPORT TYPE Technical Report		3. DATES COVERED (From - To) 01 July 2013 to 30 June 2014	
4. TITLE AND SUBTITLE MODELING THE COMBINED EFFECTS OF DETERMINISTIC AND STATISTICAL STRUCTURE FOR OPTIMIZATION OF REGIONAL MONITORING Annual Report				5a. CONTRACT NUMBER FA9453-12-C-0207	
				5b. GRANT NUMBER	
				5c. PROGRAM ELEMENT NUMBER 62601F	
6. AUTHOR(S) Vernon F. Cormier, Christopher J. Sanborn, Michele Fitzpatrick, Steven Walsh, and Nil Mistry				5d. PROJECT NUMBER 1010	
				5e. TASK NUMBER PPM00014476	
				5f. WORK UNIT NUMBER EF007739	
7. PERFORMING ORGANIZATION NAME(S) AND ADDRESS(ES) Physics Department University of Connecticut 2152 Hillside Road, U-3046 Storrs, CT 06269-3046				8. PERFORMING ORGANIZATION REPORT NUMBER	
9. SPONSORING / MONITORING AGENCY NAME(S) AND ADDRESS(ES) Air Force Research Laboratory Space Vehicles Directorate 3550 Aberdeen Avenue, SE Kirtland AFB, NM 87117-5776				10. SPONSOR/MONITOR'S ACRONYM(S) AFRL/RVBYE	
				11. SPONSOR/MONITOR'S REPORT NUMBER(S) AFRL-RV-PS-TR-2014-0163	
12. DISTRIBUTION / AVAILABILITY STATEMENT Approved for public release; distribution is unlimited. (377ABW-2014-0862 dtd 31 Oct 2014)					
13. SUPPLEMENTARY NOTES					
14. ABSTRACT The differences between earthquakes and explosions are largest in the highest recordable frequency band. In this band, scattering of elastic energy by small-scale heterogeneity (less than a wavelength) can equilibrate energy on components of motion and stabilize the behavior of the Lg wave trapped in the Earth's crust. Larger-scale deterministic structure (greater than a wavelength) can still assume major control over the efficiency or blockage of the Lg and other regional/local seismic waves. This project models the combined effects of the large-scale (deterministic) and the small scale (statistical) structure to invert for improved structural models and to evaluate the performance of yield estimators and discriminants at selected IMS monitoring stations in Eurasia. This is accomplished by synthesizing seismograms using a radiative transport technique to predict the high frequency coda (>5 Hz) of regional seismic phases at stations having known large-scale three-dimensional structure, combined with experiments to estimate the effects of multiple-scattering from unknown small-scale structure. We describe a code and preliminary tests to shoot body wave rays through general deterministic 3-D structure, including the computation of quantities required to synthesize high frequency body wave coda generated by small-scale, statistically described heterogeneity. Modifications in this period include 3-D interfaces with generalized dips and generalized 3-D reflection-transmission at the interfaces. Example regional waveform envelopes at 4 Hz are synthesized and discussed for an earthquake and explosion source in the Lop Nor region.					
15. SUBJECT TERMS seismic scattering, radiative transport, stochastic scattering, regional seismic phase amplitudes					
16. SECURITY CLASSIFICATION OF:			17. LIMITATION OF ABSTRACT Unlimited	18. NUMBER OF PAGES 26	19a. NAME OF RESPONSIBLE PERSON Dr. Robert Raistrick
a. REPORT Unclassified	b. ABSTRACT Unclassified	c. THIS PAGE Unclassified			19b. TELEPHONE NUMBER (include area code)

This page is intentionally left blank.

Table of Contents

1. Summary	1
2. Introduction.....	1
2.1 The importance of very high frequency coda modeling	1
2.2. Limitations of numerical modeling: high frequency and long range.....	2
2.3. Importance of large-scale structure and limitations of a calibration approach	2
3. Technical Approach	3
3.1. Radiative Transport.....	3
3.2. Construction of models: statistically described structure	3
3.3. Construction of models: deterministic structure	4
3.4. Synthetic Algorithm.....	4
4. Results and Discussion	9
4.1. Earth Model for Region of Interest	9
4.2. Regional Data.....	11
4.3. Synthetic Results.....	11
5. Conclusions.....	14
References	16
List of Symbols, Abbreviations, and Acronyms	18

List of Figures

1. Energy propagation visualized as a time series plot of phonon locations in a model cross section.	6
2. Seismic envelope plots produced by the Radiative3D code.	7
3. Lop Nor area and some regional seismic stations.....	10
4. Simplified Lop Nor earth model.	10
5. Lop Nor regional vertical component bandpassed waveforms.....	11
6. Synthetics from an earthquake event to MAK and WUS.....	13
7. Synthetic seismograms from an explosion recorded at MAK and WUS.....	14

1. SUMMARY

The differences between earthquakes and explosions are largest in the highest recordable frequency band. In this band, scattering of elastic energy by small-scale heterogeneity (less than a wavelength) can equilibrate energy on components of motion and stabilize the behavior of the Lg wave trapped in the Earth's crust. Larger-scale deterministic structure (greater than a wavelength) can still assume major control over the efficiency or blockage of the Lg and other regional/local seismic waves. This project models the combined effects of the large-scale (deterministic) and the small scale (statistical) structure to invert for improved structural models and to evaluate the performance of yield estimators and discriminants at selected International Monitoring System (IMS) stations in Eurasia. These tasks are approached by synthesizing seismograms using a radiative transport technique to predict the high frequency coda (>5 Hz) of regional seismic phases at stations having known large-scale three-dimensional structure, combined with experiments to estimate the effects of multiple-scattering from unknown small-scale structure. We describe a radiative transport code and report the results of its use modeling regional wave propagation in deterministic and statistical 3-D structure, including the computation of quantities required to synthesize high frequency body wave coda generated by small-scale, statistically described heterogeneity.

2. INTRODUCTION

This section provides some background and introductory material. It is largely unchanged from our earlier report, but is included to eliminate the need for readers to refer to our earlier report. In Section 3 we present the methods and procedures used to develop the code with updated tests and evaluations. Section 4 contains test our recent results and discussion. Concluding remarks are presented in Section 5.

2.1. The importance of very high frequency coda modeling

Differences in source properties between a theoretically ideal earthquake and explosion are well understood: distributed slip on a fault plane versus an approximate step-function in pressure applied to a spherical cavity deep enough for explosion containment (Brune, 1970; Mueller and Murphy, 1971). These simple theories do not incorporate dynamically triggered fault motion, complex surfaces of equivalent explosion volumes, and explosive tectonic release. Nevertheless they are good enough to accurately predict that the scalar moment of an earthquake will have much higher corner frequency in its displacement spectrum. The success of common seismic discriminants based on amplitude ratios in different group velocity windows (e.g., P/Lg) depend as much on this spectral difference as they do on differences in source depth and P and S radiation patterns (Walter et al, 2009).

High frequency Lg coda has also been shown to be useful for yield estimation (e.g., Mayeda, 1993). As frequency increases, however, it becomes increasingly difficult to

obtain perfect knowledge of small-scale structure needed to predict a seismogram of an earthquake or an explosion wiggle for wiggle. Yet even without this knowledge, simple statistical descriptions of medium properties can be used to predict the shape of high frequency Lg coda.

2.2. Limitations of numerical modeling: high frequency and long range

Given the importance of high frequencies to seismic monitoring, it would be desirable to model high frequency regional seismograms with enough computational efficiency that many structural and source models could be routinely tested and compared against observations within several hours or less. Unfortunately, even with the advance of parallel computation and increased access to large clusters of processors, numerical modeling in three-dimensional earth models rarely exceeds ranges of several hundred wavelengths for computing times less than 1 day. At 5 Hz this range is typically less than 100-200 km, which is valuable to predictions of earthquake strong ground motion, but more limited in value to nuclear monitoring where IMS stations may be 1000 km or further from regions of interest in Eurasia.

2.3. Importance of large-scale structure and limitations of a calibration approach

Given the apparent success of discriminants and yield estimators from high frequency coda with minimal knowledge of earth structure and source descriptions, one may believe that monitoring is purely a problem of calibrating coda measurements and amplitude ratios along paths to each monitoring station, applying spatial interpolators (e.g, kriging) and a model of propagation in a plane-layered medium (e.g., MDAC). Many examples have been collected in which sharp gradients in the Moho depth, mountain roots, and deep sedimentary basins have strongly affected azimuthal variations in the character and detection of regional seismic phases.

The effects of larger-scale (greater than a wavelength) structure will limit the portability of discriminants and yield estimators and limit the effectiveness of their path interpolations and calibrations. In addition to these operational concerns, a number of fundamental problems involving the interaction of large with small-scale structure have not been well investigated:

- Can large-scale structures always block the highest detectable frequency of some regional phases?
- Is there a frequency band on Earth in which the effects on regional seismograms of large-scale structure disappear?
- How important is small-scale structure in the vicinity of large-scale structure?
- Is anisotropy of the scale-lengths of small-scale structure (horizontally or vertically stretched heterogeneity) important to regional phase propagation?

By combining the effects of large-scale and small-scale structure in a computationally efficient 3-D method of seismogram synthesis based on the radiative transport approach,

our project seeks to determine small-and large-scale 3-D structure in the vicinity of selected Eurasian IMS stations by matching the coda of very high frequency (> 5 Hz) regional phases. The results of this modeling will be used to optimize coda-based yield estimators and discriminants as a function of azimuth to these stations.

3. TECHNICAL APPROACH

3.1. Radiative Transport

Radiative transport seeks to model the diffusive transport of energy through processes of multiple scattering in a medium having random fluctuations in physical properties. Its earliest and most extensive applications are to the propagation of electromagnetic waves, especially to the description of stellar images and scintillation (Chandrasekhar, 1960). Wu (1985) introduced radiative transport to seismology, modeling the coda, or envelope of energy, starting and following elastic P and S waves. By including multiple-scattering, radiative transport improved upon the single scattering, Rayleigh-Born, model of seismic coda introduced by Aki and Chouet (1975). An early significant result of Wu's work with radiative transport is that multiple scattering often becomes the dominant mechanism controlling coda shapes at frequencies above 5 Hz on Earth, explaining a spindle-shaped (lunar-like) coda observed in this frequency band. Reviews of seismic radiative transport modeling include the text by Sato and Fehler (1998) and a monograph by Margerin (2004). Przybilla, et al. (2009) has compared the method against finite-difference synthetics in 2-D, validating body wave coda predictions of the radiative transport method.

3.2. Construction of models: statistically described structure

Frankel and Clayton (1986) demonstrated how earth models can be constructed that have a specified heterogeneity spectrum. The procedure consists in having perturbations at knot points driven by a random number generator, Fourier transforming the spatial model into the wavenumber domain, filtering by a desired wavenumber spectral shape, and inverse Fourier transforming back to space.

Since Frankel and Clayton's original work, advances have occurred in statistical characterization and understanding of small-scale geologic heterogeneity. Goff et al. (1994) described a procedure by which models having the spatial statistics of polycrystalline or multi-modal assemblages of rocks can be generated. Work beginning with Levander et al. (1994) and Pullammanappallil et al. (1997) makes it possible to formulate statistical models for common sedimentary and metamorphic formations. Model statistics can be modified as needed to reproduce the three-component behavior of the coda of regional seismic phases. Strong emphasis is placed on correctly characterizing the statistics of small-scale heterogeneities in the upper, highly heterogeneous, 5 km of the earth. Small-scale statistics affect the partitioning of P and S energy on the three-components of motion by the effects of scattering near the source and receiver and hence the performance of discriminants is tuned to differences in sources occurring at the depths of contained nuclear tests.

3.3. Construction of models: deterministic structure

Lateral variations in crustal thickness, basin depths, mountain roots, and lateral tectonic transitions significantly affect the phases used for discrimination and detection. One example is the study by Pedersen et al. (1998), who explain anomalous Rayleigh to Love mode conversion from Lop Nor explosions by changes in crustal thickness at the boundary of the Tarim Basin and Tian Shan mountain belt. Moho topography and basin thickness can also strongly affect the propagation of Lg (Cormier and Anderson, 2004). The scale of these types of lateral structural variations is often large enough to be resolvable by local and regional reflection and refraction experiments, gravity and magnetic data, regionalization by surficial geology, and global surface wave inversions. Hence, we refer to these types of structures as deterministic. The types of data used to infer deterministic structure are collected at widely different spatial scales, presenting a challenge to the parameterization of a three-dimensional model appropriate for a region surrounding a particular seismic station. The parameterization should be flexible enough to be specified at high resolution where data is available and at lower resolution where it is not. Resolution should be high to describe features important to regional wave propagation, such as Moho and basin topography, but can be lower near interfaces having smaller velocity contrasts and lower with increasing depth in the mantle, where heterogeneity power decreases.

3.4. Synthetic Algorithm

We are developing a 3-D radiative transport code for synthetic seismogram generation called Radiative3D. Radiative3D is a new code that builds upon and augments two existing codes, namely Raytrace3d (Menke, 2002) and PSPhonon (Shearer and Earle, 2004; 2008). Raytrace3D solves ray propagation in a 3-D velocity model, and PSPhonon performs radiative transport, including scattering, in a 1-D layered-earth model. Our code performs both tasks in a full 3-D model.

Radiative transport theory treats seismic energy as composed of discrete energy packets leaving elements of solid angle surrounding a source region, and uses ray theory to trace the paths of these energy packets (phonons) through a deterministic velocity model. Travel time, path integrated intrinsic attenuation, and polarization of particle motion are tracked as the phonons propagate. Seismic energy is finally collected and tabulated into temporal and spatial bins when they reach the surface of the model or some other point-of-interest in the model. This allows the generation of synthetic seismograms at specified model locations.

The radiative transport approach has several advantages and some short-comings which differentiate it from other approaches. In particular, radiative transport:

- Requires “spraying” a sufficient quantity of phonons from the source event, covering a range of take-off angles designed to mimic either earthquake or explosion energy release.

- Is generally faster than solving the full wave equation.
- Uses ray theory to model energy transport through large-scale “deterministic” structure (valid when wavelengths are sufficiently small compared to length scales of the deterministic structure being modeled).
- Effects of small-scale structure are modeled using Monte Carlo methods by implementing a statistical scattering model.
- The Lg wave and its coda are modeled by S body waves, multiply reflected at critical incidence from the Moho, multiply scattered and trapped in the crust.
- The Pn wave and its coda are modeled by P waves interacting with and turning beneath the Moho and scattered by statistical structure surrounding the Moho.
- The Rg wave cannot be properly represented as a fundamental model mode Rayleigh wave having frequency-dependent, exponentially decaying, energy beneath the free surface. This limitation, however, is mitigated by observations that very high frequency (>2 Hz) Rg is normally absent in local/regional seismograms beyond 200 km range due to strong scattering by surface topography along its path.

The development, testing, and validation of Radiative3D includes a number of steps, which are discussed below with their related results. Steps discussed in last year’s report include:

- The ability to spray P- and S-polarized phonons from a defined source according to a pattern specified by a six-element moment tensor, which can describe both explosion and shear-dislocation point-source events;
- The ability to propagate phonons through a whole-space elastic medium of constant seismic velocity;
- The ability to simulate a scattering event after propagating a randomly chosen distance selected from a mean-free-path distribution determined by the scattering parameters of the medium;
- The ability to modify the trajectory and polarization of the phonon at a scattering event according to the scattering functions of Sato and Fehler (1998);
- The ability to collect and record the seismic energy of the phonons at plane interfaces located a specified distance from the source and resolve it into three components of motion, allowing the generation of synthetic seismic envelopes.

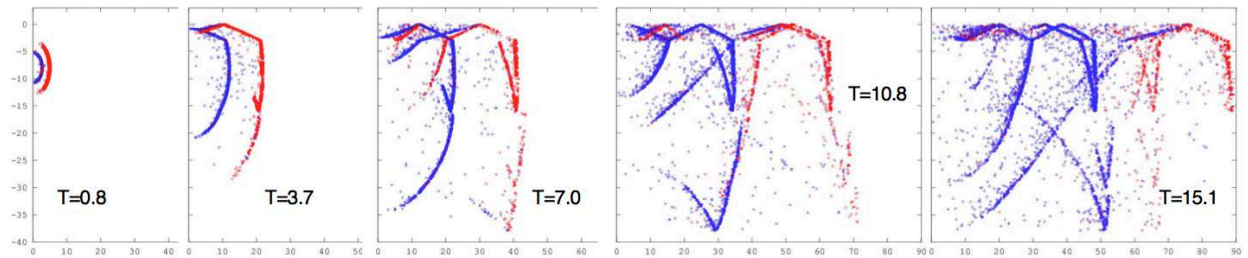
3.4.1. Visualizing Output

Radiative3D produces output suitable for visualization with external tools. The output capabilities fall into two major categories: (1) event reporting, and (2) seismic energy binning. Event reporting means reporting the progress of individual phonons in a play-by-play manner. Examples of “events” in this context include: generation, scattering, crossing a model boundary, free-surface or discontinuity interface reflection and transmission, etc. When these events are analyzed in post-processing, detailed pictures of energy propagation can be constructed. One of the first visualization tools developed was

a GNU Octave script to produce videos illustrating P and S energy propagation in the Earth model.

Figure 1 shows energy propagation visualized as a time series plot of phonon locations in a model cross section. Red dots represent P phonons, blue dots represent S phonons. Reflection and refraction occurs at interfaces between model layers at which velocities are discontinuous. Conversions between P and S polarization are driven by both scattering and reflection/transmission events.

Earthquake Time-Series:



Explosion Time-Series:

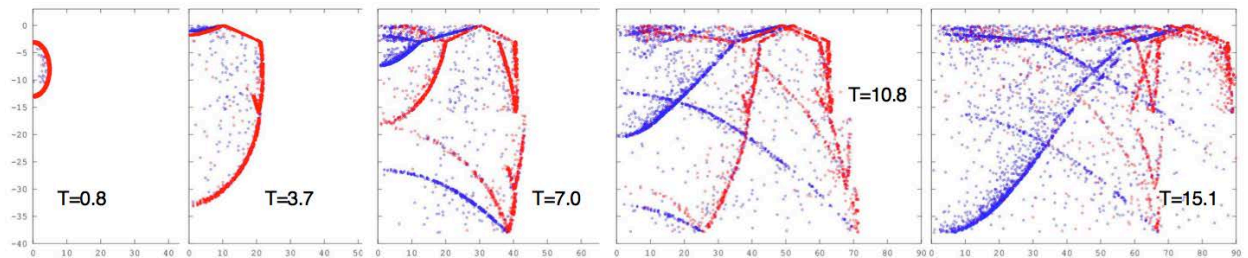


Figure 1. Energy propagation visualized as a time series plot of phonon locations in a model cross section. *Note the initial absence of the S wavefronts (blue) in the explosion time-series and its progressive development with time due to multiple scattering and interaction with the free surface.*

3.4.2. Seismometer Output

The other form of output which can be analyzed for quantification or visualization is binned seismic energy. Radiative3D allows for the placement of virtual seismometers along any surface designated as a collection surface. Whenever a phonon interacts with a collection surface within a specified gather radius of a seismometer, the energy of that phonon is collected by the seismometer, decomposed into three cartesian energy axes, and binned into time windows. At the end of simulation, these energy bins are output and can be interpreted as seismic energy traces, suitable for making envelope plots. Traces from multiple seismometers arranged in a linear array can be combined to make travel-time curves.

Figure 2 shows two seismic envelope plots produced by the Radiative3D code. The traces represent 4.0 Hz phonon energy arriving at a virtual seismometer approximately 900 km from a hypothesized earthquake source (left) and explosion source (right) synthesized in a 3-D model of the Lop Nor region having a simple deterministic and trial statistical structure.

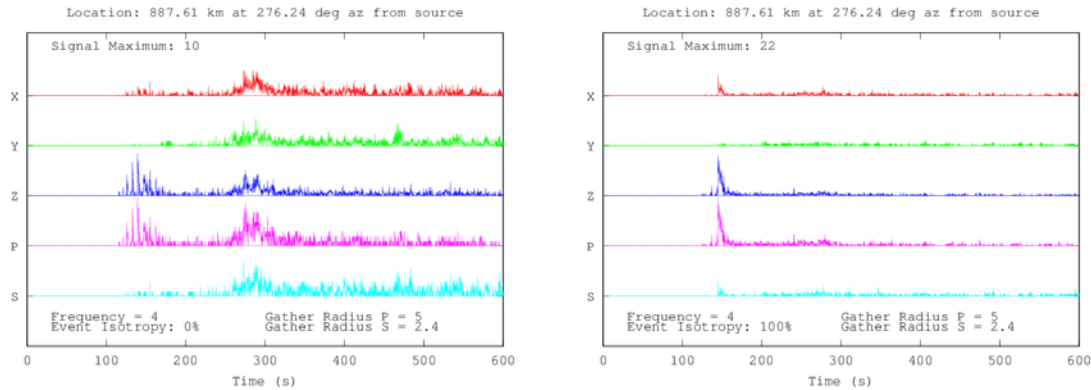


Figure 2. Seismic envelope plots produced by the Radiative3D code. *Traces are shown for components of motion NS (Y), EW (X), and vertical (Z) and wave type (P or S) arriving at the receiver.*

3.4.3. New Features Complete:

In addition to features reported in last year's report, the following new features are fully or substantially complete as of this writing:

Layered multi-cell Earth models:

While full-3D Earth models based on tetrahedral model cells are not yet supported, an intermediate cell type based on stacked cylinders is supported and functional for simulating layered-Earth models. Partial-3D functionality is available because the interfaces between adjacent cylinders can be given an arbitrary inclination. This means that first-order lateral variations, such as a sloped Moho can be modeled.

Reflection/Transmission scattering at discontinuity interfaces:

Free-surface reflections, as well as sharp velocity discontinuities (such as at the Moho layer), require special treatment of ray propagation. Much like the radiation patterns of scattering from small-scale volumetric inhomogeneities, a ray's interaction with an interface across which seismic velocities and/or material densities abruptly change can be thought of as a form of scattering radiation pattern. For a given incident ray, there are up to four different outgoing ray directions, and two different ray types (P and S), with special care being necessary to correctly transform the S-polarization angle. Aki and Richards (1980) develop a set of 20 scattering coefficients that cover all possibilities between incoming P and S waves and their associated transmitted or reflected P or S outgoing waves. These coefficients quantify the amplitude and phase of the outgoing waves, which is used by Radiative3D to compute probabilities of an incoming ray transforming into the corresponding outgoing ray type. This allows for the modeling of

reflection (at a free surface or interface) and transmission (interface) of rays with corresponding possibility of transformation between P and S polarization types. This feature has been recently completed in the Radiative3D codebase.

3.4.4. Some Notable Features Not-Yet Complete:

Software development is ongoing, and while we have reached a state where certain studies of real-world significance can be undertaken with the code as-is, there still remain some features to be developed before we reach full target functionality. The most significant of these are:

Tetrahedral Model Cells:

Three-dimensional Earth models, having fully general spatial gradients of velocity and density within layers need to be discretized in some fashion. The method we have chosen is to divide the model into tetrahedral cells inside of which the Earth parameters are analytically specified. A tetrahedron is the polyhedron with the minimum number of vertices needed to specify a three-dimensional volume, which allows for straightforward approaches to dividing space into cellular components. Another advantage of tetrahedra, (over, e.g., rectangular prisms), is that Earth parameters specified on the four vertices allows unique and complete specification of the properties in terms of linear gradients throughout the volume of the cell.

Much of the infrastructure for cellular model discretization is already complete in the code, and is utilized in the layer-celled structure already supported in the code. Implementing cells with tetrahedral geometry remains primarily an implementation detail at this point.

Velocity Gradients:

In a uniform-velocity medium, ray paths are straight lines. In the real Earth, rays can follow curvilinear paths. The plan for Radiative3D is for velocities to be specified as first-order gradients, resulting in paths which are circular arcs within a given model cell. This allows for a much more natural representation of real Earth structure, and lessens the detail needed to represent that structure. At present Radiative3D supports only uniform velocities (gradients on the macro level can be represented as a multicellular stair-step model). The next development step of Radiative3D will be to implement support for velocity gradients. This step will naturally follow the implementation of tetrahedral model cells, since this geometry allows the unique specification of the gradients by specifying known velocities on the cell vertices.

3.4.5. Features Not Currently Targeted:

In addition to the code features detailed above, another feature, not currently targeted for development, remains within feasible reach of the codebase as it now stands, and may provide a starting point for future work. In particular, while Radiative3D currently

produces seismic envelope plots, it is technically possible to produce full-waveform seismograms by tracking not only the amplitude, but also the phase, of each phonon as it propagates through the model. By binning the seismic energy as amplitude phasors rather than energy scalars, full seismograms, rather than envelopes, can be produced. Phase tracking through direct propagation is trivial, as it is proportional to the product of frequency and travel time. Slightly more intricate are the phase shifts that result from scattering events, and from reflection/transmission interactions with discontinuity or free-surface interfaces. However, these phase factors are actually already calculated by the codebase when it calculates scattering and reflection/transmission probabilities. Adding the accounting necessary to track cumulative phase through a phonon lifetime would be a very tractable problem.

4. RESULTS AND DISCUSSION

4.1. Earth Model for Region of Interest

We originally planned to focus our study on the area in the vicinity of the NIL seismic station. We discovered that while there were many earthquakes with regional seismograms in that area, regional explosion data were severely lacking. We next planned to use regional explosion data from the Semipalatinsk Test site (STS) in Kazakhstan as received at the Borovoye (BRV) Geophysical Observatory in Kazakhstan. Currently there are few earthquake waveforms in that area to compare with explosion waveforms. (This may be alleviated in the near future by the LDEO digitization project of analog seismograms recorded by regional and PNE associated networks in the former USSR). We decided to switch to the Lop Nor explosion area since there were both explosion and earthquake waveforms in the same area, in addition to the availability of detailed maps of regional wave propagation efficiencies by LANL. Lop Nor is located near the southeastern side of the Tien Shan, a region of moderate earthquake activity and contemporary horizontal compressive stress in the earth's crust, which proves to be of significance in the discrimination of earthquakes from nuclear explosions in that region. Sykes and Nettles (2009) found that more than half of the total numbers of earthquakes in the Reviewed Event Bulletin (REB) of the IMS that occurred within 100 km (62 mi) of six test sites from 2000 through 2008 occurred near Lop Nor.

Figure 3 shows the area we're currently investigating. The Chinese station Urumqi (assigned the station code WMQ by seismologists) is about 2.15° (250 km or 156 mi) from Lop Nor. MAK and WUS are $\sim 6.85^\circ$ from Lop Nor. For the earthquake and explosion data we use seismograms from events found using the Incorporated Research Institutions for Seismology (IRIS) web site.

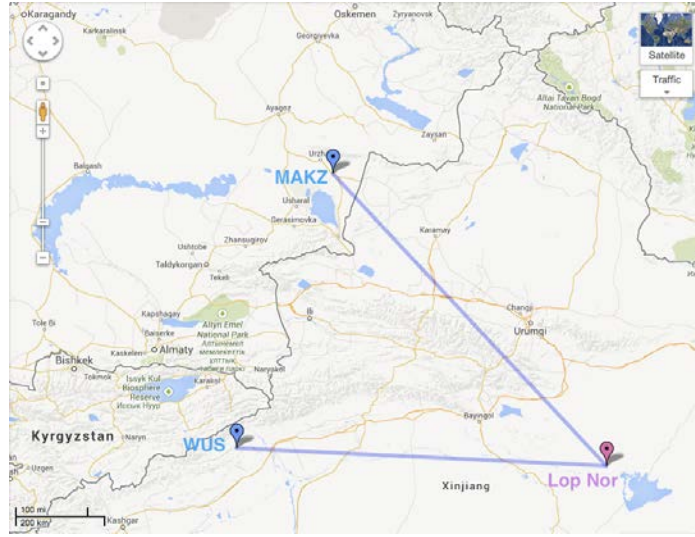


Figure 3. Lop Nor area and some regional seismic stations.

Although we have not constructed a detailed 3-D earth model for this region, we constructed a simple 3-D model to begin synthetic tests. The model was constructed of layers of uniform velocity, with dipping planes separating the layers (Figure 4). Current functionality in Radiative3D allows these interface planes to take on arbitrary 3-D orientation. Depth profiles from CRUST2.0 topographic elevations, and Moho depths at three locations (Lop Nor, MAK, and WUS) were used to locate and orient the planes.

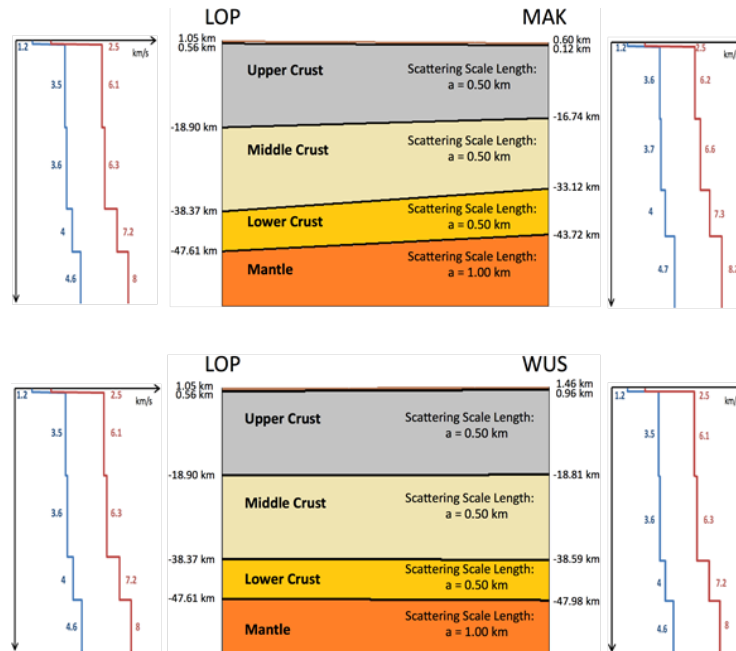


Figure 4. Simplified Lop Nor earth model. *Note a thin sediment, low P and S velocity, layer is included.*

4.2. Regional Data

Figure 5 shows some waveform examples from the Lop Nor region. The data come from an explosion at the Lop Nor site as recorded at station MAK at great circle distance 6.85° and an earthquake in the same area recorded at both MAK and WUS. WUS is approximately at the same distance from Lop Nor as MAK but in at different azimuth. The left column in Figure 5 shows the data bandpass filtered 1-2 Hz and the right column shows filtering 6-8 Hz. Not only are there differences between the earthquake and explosion data at MAK, there are also differences between the earthquake traces at MAK and WUS. We plan to use our synthetics to explore and understand these differences from effects of both large- and small-scale 3-D structure.

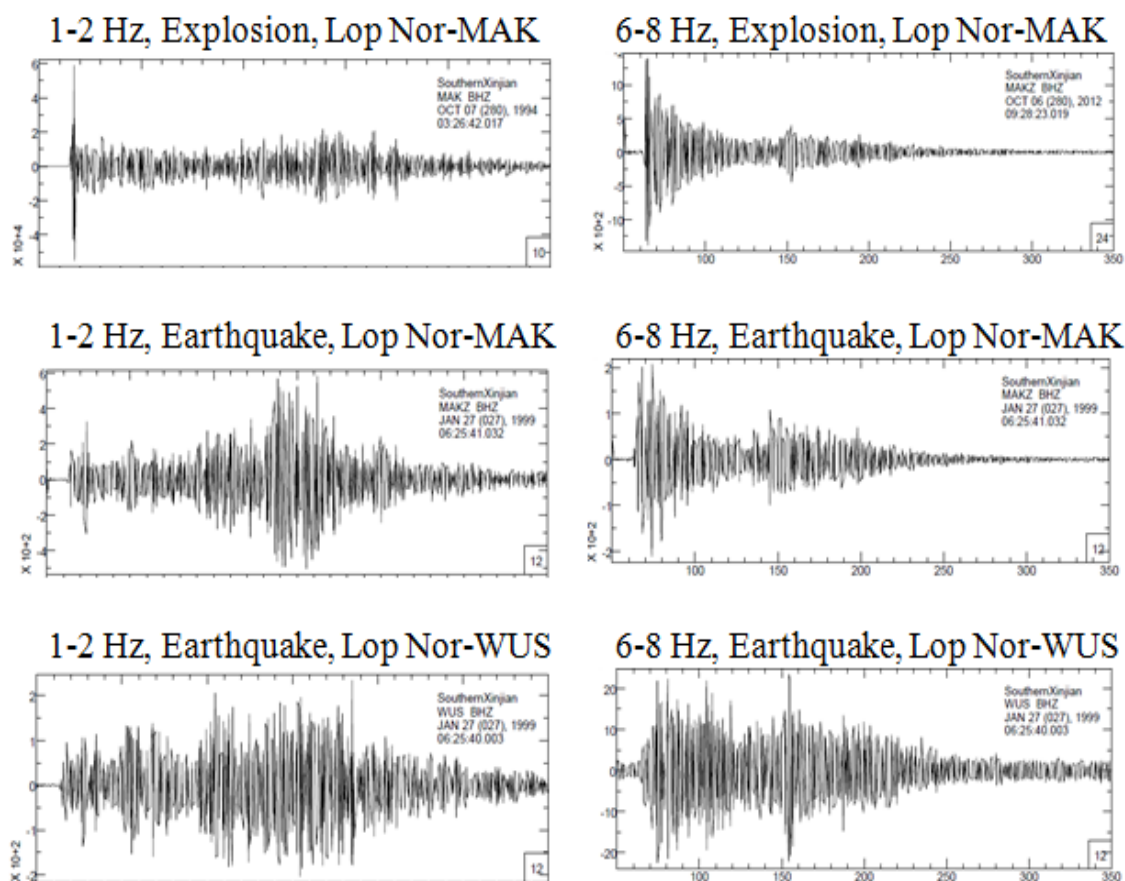


Figure 5. Lop Nor regional vertical component bandpassed waveforms.

4.3 Synthetic Results

We have produced envelope and travel-time synthetics in Radiative3D using a simplified Earth model serving as a stand-in for more complex models to be supported in future revisions as work on Radiative3D comes to completion. The Earth model used is a layered model consisting of layers of spatially uniform parameters (velocity, density,

scattering parameters). The planar interfaces separating the layers need not be parallel, and in fact can take on arbitrary orientations. We have taken advantage of this freedom to construct a first-order approximation of the topography (both surface and subsurface, e.g., Moho) in the region of the Lop Nor nuclear test site. Using known elevations of Lop Nor and seismic stations MAK and WUS, along with Moho depths from the Cornell Moho model and layer profiles from CRUST2.0 at those same locations, we located and oriented a set of four crustal layers (sediments, upper, middle, and lower crust, and the top layer of the mantle). We also defined an additional 16 mantle layers from AK-135, to a depth of 859 km. These layers served as a model in which to run early test synthetics.

The model assumed a minimum characteristic scale length in an exponential autocorrelation of heterogeneities of 0.50 km in the crust, 1.00 km in the mantle, and 0.25 km in the thin sediments layer. (An exponential autocorrelation provides a white heterogeneity spectrum up to the minimum scale length, at which the heterogeneity power decays as k^{-2} with increasing wave number k). Scattering strengths, defined as the fractional velocity perturbations that characterize the heterogeneity, were 0.01 in the crust, 0.008 in the mantle, and 0.012 in the sediments layer. Figure 4 shows cross-sections illustrating the crustal layers of the test model along the two paths.

Situated within the model we place two arrays of 160 virtual seismometers each along the paths of Lop Nor to WUS and Lop Nor to MAK. These arrays collect and bin the phonon counts to produce synthetic envelopes and travel time curves.

Synthetic envelopes are for a frequency of 4.0 Hz and an assumption that all phonons originate at time $t = 0$. (Temporally complex events can be simulated in post-processing by convolution with a source time function.) We modeled two distinct source mechanisms parameterized by moment tensor elements. One mechanism was a pure isotropic event meant to simulate an idealized explosion, and the other was a pure shear event to simulate an earthquake. We set the depth of the explosion event to 2.0 km below the surface, and the depth of the earthquake event to 42.0 km below the surface, comparable to some of the larger magnitude earthquakes recorded in the region. The simulation consisted of the spraying of 200 million phonons from the event source at probabilistically chosen take-off angles selected from a discrete set of 5.2×10^6 possible take-off angles roughly evenly spaced throughout a unit sphere (no preferred direction). The source radiation pattern is determined via relative probability amplitudes for each take-off angle computed from moment tensor elements at program initialization.

Figure 6 shows synthetics from the earthquake along the two paths. The travel-time plots show two major divisions of energy arrival, with the lowest slope (time/range) arrival representing the Pn-wave arrival and the higher slope arrival representing the Sn-wave and succeeding Lg coda. We believe the banding in each arrival is the result of surface to Moho multiples comprising Lg, but this is unconfirmed as yet. There is a stark difference in the relative amplitude of the P and S arrivals between the two paths. We believe the majority of this difference is explainable via the source radiation pattern and that only minor visible differences are explained by topographical differences between the Lop Nor to WUS and Lop Nor to MAK paths.

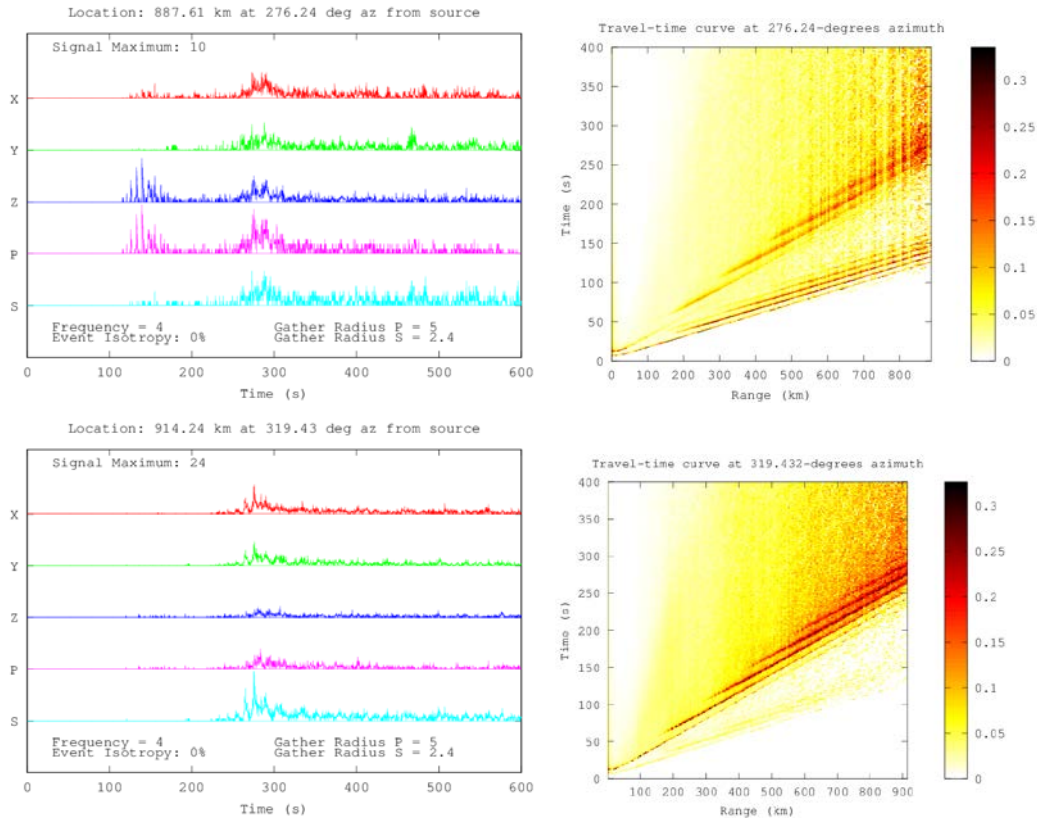


Figure 6. Synthetics from an earthquake event to MAK and WUS.

Figure 7 shows synthetics from the explosion event along the same two paths. The most noticeable difference between these and the earthquake synthetics is the absence of a coherent S-wave front. Also absent is any obvious banding in the P-wave arrival, which is curious, but may be a result of the much shallower source depth, resulting in a stronger direct arrival and suppression of surface multiples due to oblique incidence of the surface reflections. Differences between the two paths are harder to see in the travel-time plots, but can be seen more readily in the envelope plots. Since the event source is isotropic, any differences in energy arrival between the paths must result from path differences in topography. The path from Lop Nor to MAK is more sloping and the path from Lop Nor to WUS is more flat.

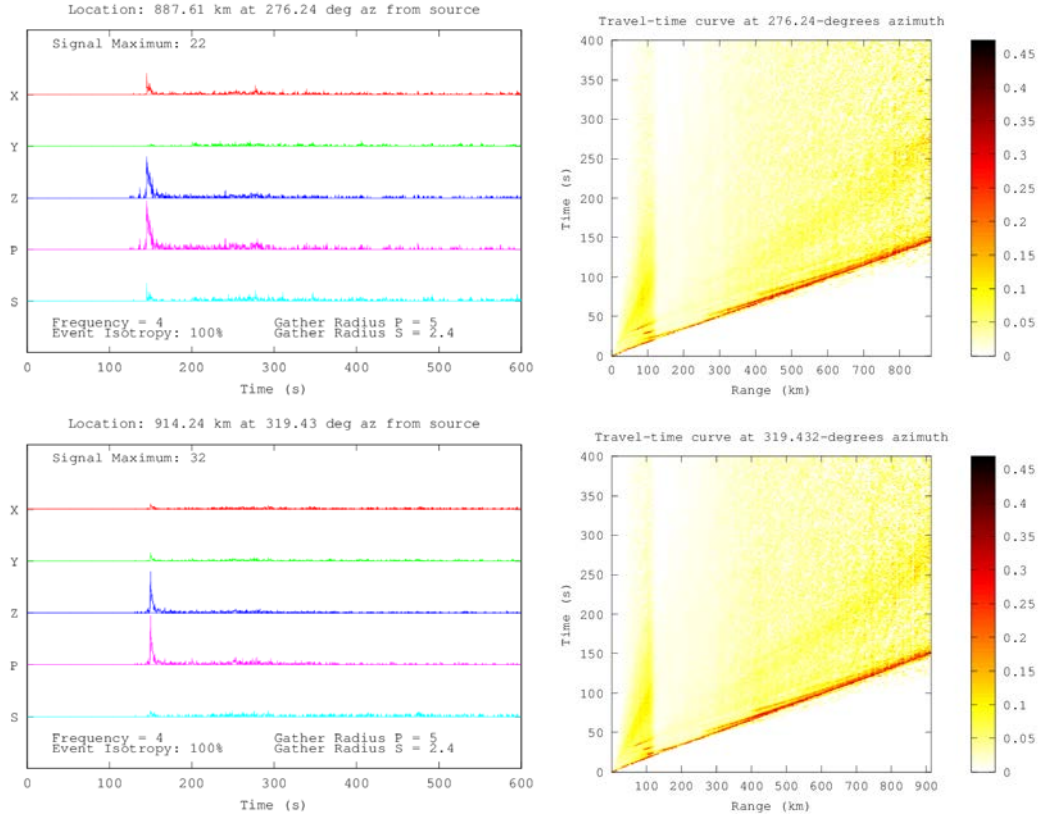


Figure 7. Synthetic seismograms from an explosion recorded at MAK and WUS.

5. CONCLUSIONS

We have continued development of a code to shoot body wave rays through general deterministic 3-D structure, including the computation of quantities required to synthesize high frequency body wave coda generated by small-scale, statistically described heterogeneity. Modifications in this period include layer boundaries having generalized dips and the treatment of reflection-transmission at 3-D boundaries. Features to be added in the next reporting period will include generalized 3-D spatial gradients within layers, and the effect of path integrated intrinsic attenuation. Spatial velocity gradients beneath the Moho will be particularly important for predicting the efficiency of Pn and Sn propagation.

Coda envelopes can be plotted in several styles with different emphases: as a function of time and component of motion at a single station, as a function of distance and time to assist in travel-time picking and travel-time uncertainty estimates, or as snapshots in time as a function of depth and range to understand the evolution of P and S energy and the homogenization of the radiation pattern.

The availability of both explosion and earthquake waveforms, detailed maps of regional phase efficiency, and the existence of many well-constrained 3-D deterministic structural models derived from transportable array studies makes the Lop Nor region an

ideal region to implement our modeling technique. Our goals will include the modeling of effects of the unknown small-scale structure and its associations with regional geology and tectonics, and an effort to explain the LANL mapped patterns of regional phase propagation efficiency.

References

- Aki, K. and Chouet, B., "Origin of coda waves: Source, attenuation, and scattering effects," *J. Geophys. Res.*, **80**, 1975, pp. 3322-3342.
- Aki, K. and Richards, P.G., Quantitative Seismology, Theory and Methods, Vol. I and II. Freeman, New York, N.Y., 1980.
- Brune, J.N., "Tectonic Stress and the Spectra of Seismic Shear Waves from Earthquakes," *J. Geophys. Res.*, **75**, 1970, p. 499.
- Chandrasekhar, S., Radiative Transfer, Dover, New York, N.Y., 1960.
- Cormier, V.F. and Anderson, T.S., "Efficiency of Lg propagation from SmS ray tracing in three-dimensionally varying crustal waveguides," *Pure and Appl. Geophys.*, **161(8)**, 2004, pp. 1613-1633.
- Frankel, A. and Clayton, R.W., "Finite difference simulations of seismic scattering: implications for the propagation of short-period seismic waves in the crust and models of crustal heterogeneity," *J. Geophys. Res.*, **91**, 1986, pp. 6465-6489.
- Goff, J.A., Holliger, K., and Levander, A., "Modal fields: A new method for characterization of random seismic velocity heterogeneity," *Geophys. Res. Letters*, **21**, 1994, pp. 493-496.
- Levander, A., England, R.W., Smith, S.K., Hobbs, R.W., Goff, J.A., and Holliger, K., "Stochastic characterization and seismic response of upper and middle crustal rocks based on the Lewisian Gneiss Complex, Scotland," *Geophys. J. Int.*, **119**, 1994, pp. 243-259.
- Margerin, L., "Introduction to radiative transfer of seismic waves," In: Seismic Data Analysis and Imaging With Global and Local Arrays, AGU Monograph Series, 2004.
- Mayeda, K., " m_b (LgCoda): A stable single station estimator of magnitude," *Bull. Seism. Soc. Am.*, **83**, 1993, pp. 851-861.
- Menke, W., *Case Studies of Seismic Tomography in a Regional Context*, 2002, <http://www.iris.edu/software/downloads/plotting/>.
- Mueller, R.A. and Murphy, J.R., "Seismic characteristics of underground nuclear detonations: Part I. Seismic spectrum scaling," *Bull. Seism. Soc. Am.*, **61**, 1971, pp. 1675-1692.
- Pedersen, H.A., Avouac, J-P., and Campillo, M., "Anomalous surface waves from Lop Nor nuclear explosions: observations and numerical modeling," *J. Geophys. Res.*, **103**, 1998, pp. 15,051-15,068.
- Przybilla, J., Wegler, U., and Korn, M., "Estimation of crustal scattering parameters with elastic radiative transfer theory," *Geophys. J. Int.*, **178**, 2009, doi:10.1111/j.1365-246X.2009.04204.x.
- Pullammanappallil, S., Levander, A., and Larkin, S.P., "Estimation of stochastic crustal parameters from seismic exploration data," *J. Geophys. Res.*, **102**, 1997, pp. 15,269-15,286.
- Sato H. and Fehler, M.C., Seismic Wave Propagation and Scattering in the Heterogeneous Earth, Springer-Verlag, New York, N.Y., 1998.
- Shearer, P.M. and Earle, P.S., "The global short-period wavefield modeled with a Monte Carlo seismic phonon method," *Geophys. J. Int.*, **158**, 2004, pp. 1103-1117.

- Shearer, P. M. and Earle, P.S., In: Advances in Geophysics, Volume 50: Earth Heterogeneity and Scattering Effects on Seismic Waves, H. Sato and M.C. Fehler (ed.), 2008.
- Sykes, L.R. and Nettles, M., “Dealing with Hard-to-identify Seismic Events Globally and those near Nuclear Test Sites,” Poster presented at the International Scientific Studies Conference, Comprehensive Nuclear Test Ban Treaty Organization, Vienna, Austria, 2009. Available at: [http://www.ctbto.org/fileadmin/user_upload/ISS_2009/Poster/SEISMO-26J%20\(US\)%20-%20Lynn_Sykes%20and%20Meredith_Nettles.pdf](http://www.ctbto.org/fileadmin/user_upload/ISS_2009/Poster/SEISMO-26J%20(US)%20-%20Lynn_Sykes%20and%20Meredith_Nettles.pdf).
- Walter, W.R., Matzel, E., Pasyanos, M.E., Harris, D.B., Gok, R., and Ford, S.R., “Empirical observations of earthquake-explosion discrimination using P/S ratios and implications for the sources of explosion S-waves,” 29th Monitoring Research Review: Ground-based Nuclear Explosion Technologies, report of contract no. W-7405-ENG-48, 2009.
- Wu, R.S., Multiple scattering and energy transfer of seismic waves — separation of scattering effect from intrinsic attenuation — I. Theoretical modelling. Theoretical modeling, *Geophys. J. R. Astr. Soc.*, **82**, 1985, pp. 57-80.

List of Symbols, Abbreviations, and Acronyms

AFRL	Air Force Research Laboratory
IMS	International Monitoring Station
IRIS	Incorporated Research Institutions for Seismology
LANL	Los Alamos National Laboratory
LDEO	Lamont-Doherty Earth Observatory
PNE	Peaceful Nuclear Explosion

DISTRIBUTION LIST

DTIC/OCP 8725 John J. Kingman Rd, Suite 0944 Ft Belvoir, VA 22060-6218	1 cy
AFRL/RVIL Kirtland AFB, NM 87117-5776	2 cys
Official Record Copy AFRL/RVBYE/Dr. Robert Raistrick	1 cy

This page is intentionally left blank.